Thermal Degradation Studies on Polyaniline–Polypyrrole Copolymers Prepared by Microemulsion Methods

A. Prasannan · N. Somanathan · Po-Da Hong

Abstract Solvent- and water-based microemulsions of aniline and pyrrole copolymers were synthesized, and the thermal degradation properties of the copolymers were studied. The morphology of the copolymers prepared using solvent-based microemulsions containing 80 % aniline in the feed showed highly oriented, crystalline, ordered long nano-fibers which were even more structured than that of pure aniline prepared by the same method. The influence of the degree of crystallinity calculated from X-ray diffraction and morphology had an overlap with thermal degradation and activation energies of different transitions. Copolymers prepared with water-based microemulsions were thermally less stable than the ones prepared using solvent-based microemulsions. The concentration of pyrrole and aniline mutually influenced the thermal properties of the copolymers.

1 Introduction

Conducting polymers possess the advantage of retaining the processibility and mechanical properties of polymers along with the electronic, electrical, and optical properties shown by metals. Polypyrrole and polyaniline have gained their popularity

A. Prasannan · P.-D. Hong
Graduate Institute of Materials Science and Engineering, National Taiwan University of Science and Technology, Taipei 106, Taiwan

N. Somanathan (✉)
Polymer Laboratory, Central Leather Research Institute, Chennai 600 020, India
e-mail: nsomanathan@rediffmail.com

by exhibiting good thermal and oxidative stability. A combination of the superior properties of the above polymers in the form of composites, such as copolymers [1–5] is of recent interest. It is well known [6] that the properties of materials depend not only on their chemical structure, but also on their morphology. The latter is very much influenced by the method and conditions of preparation of the polymer. It is well known that microemulsion polymerization is very effective in producing polymer particles in the size range of 5 nm to 100 nm. A microemulsion is an organized microheterogeneous system, which provides a large interfacial area with lower viscosity. It has been shown that the orientation behavior of surfactants can be detected in a microemulsion system in which the monomer chains are aligned. Self-assembling behavior results in molecular ordering of polymers in microemulsions [7,8].

Surfactants have been used as additives in the polymerization of aniline and pyrrole [9] to affect the locus of polymerization by using emulsion [10] or inverse emulsion [11,12] pathways, and thus to modify the molecular and supramolecular structure of the resulting polymers. It also helps to improve the properties of the polymers with respect to conductivity, stability, and processibility. The latter approach implicitly expects that a surfactant becomes incorporated into a conducting polymer. The presence of surfactant micelles controls the distribution of the reactants between the micellar and aqueous phases, thus altering the course of polymerization. The hydrophobic part of the surfactant molecules may adsorb on the produced conducting polymer, the surfactant thus becoming a part of the resulting material. The morphology and composition of the micelles are strongly affected by the nature of the dopant and reaction conditions including the concentrations of the dopant, oxidant, solvent, and monomer as well as the molar ratio of the dopant and oxidant as mentioned earlier.

Thermal properties of the conducting polymers are much affected by the crystallinity which is controlled by the orientation order of the molecules. The thermal stability of conducting polymers is important since heat is generated during conduction and affects the conductivity and thermal degradation of the polymers. Knowledge of the environmental stability and degradation behavior is a prequalification for use of polymer films in many practical applications [13]. Most of the investigations on thermal degradation of polyaniline are carried out by thermo-gravimetric and differential scanning calorimetric analyses [14–17]. Despite considerable research [18–21], thermal degradation of polypyrrole and polyaniline composites are still not clearly understood as the presence of counter anions and their interaction with the polymer affects the degradation process.

In the present study, water- and solvent-based microemulsion copolymers of aniline and pyrrole at different compositions were prepared and the influences of the co-monomer composition and preparation conditions on the thermal behavior of the copolymers are studied in detail. Since these conducting emulsions were designed towards application in novel electrodeposition techniques like powder coating for nonconducting surfaces, thermal degradation properties were found to be an important parameter for the above process. Thermal properties of two series of polymers prepared with different conditions of solvent that critically affect the properties were compared. In the above preparation, different types of initiators are used for the above series of polymers in order to have good polymer formation and conductivity for the above-mentioned end use application.

Table 1 Concentration and ratio of co-monomer, initiator used for SBMEs

Copolymer	Monomer composition in the feed		Mass of initiator (mmol)	Total monomer Concen. (mmol)
	Aniline hydrochloride (mass%)	Pyrrole (mass%)		
SBMEI	0	100	0.29	1.26
SBMEII	20	80	0.29	1.26
SBMEIII	40	60	0.29	1.26
SBMEIV	50	50	0.29	1.26
SBMEV	60	40	0.29	1.26
SBMEVI	80	20	0.29	1.26
SBMEVII	100	0	0.29	1.26

2 Experimental

2.1 Preparation of Polyaniline–Polypyrrole (PANI–PPy) Solvent-Based Microemulsion (SBME)

Aniline and pyrrole were freshly distilled and preserved in amber colored bottles. A calculated quantity of aniline was added to a calculated quantity of 0.1 N hydrochloric acid. To this, a calculated quantity of pyrrole was added (Table 1). Then 2.6 ml of water, 51.3 ml of cyclohexane, 6.1 ml of 1-butanol, and 2.4 g of sodium dodecyl sulphate (SDS) were mutually dissolved to form an emulsion. The above solvent mixture of 25 ml was used to dissolve a known quantity of monomer. To this solution, 0.29 mmol of ammonium persulphate (APS) dissolved in 35 ml of the above-mentioned solvent mixture was added dropwise for an hour at room temperature under constant stirring. The contents were stirred further to obtain a microemulsion which changes from green to bluish black. The copolymers were precipitated using methanol, washed with water, methanol, and acetone, and dried in vacuum. The amounts of monomer and oxidizing agent, used for the preparation of solvent-based microemulsions of copolymers are shown in Table 1.

2.2 Preparation of Polyaniline–Polypyrrole (PANI–PPy) Water-Based Microemulsion (WBME)

A calculated quantity of aniline was added to a calculated quantity of 0.1 N hydrochloric acid. To this, pyrrole was added (Table 2). Then 0.007 mol of SDS was dissolved in 100 ml of distilled water with vigorous stirring to obtain an emulsion system. Ferric chloride (0.026 mol), pre-dissolved in 10 ml of distilled water, was added to the above emulsion at room temperature, and the contents were stirred during the reaction. Copolymers obtained by the above method were precipitated, washed, and dried as mentioned earlier.

Thermo-gravimetric analyses (TGA) of the above-prepared copolymers (using solvent- and aqueous-based methods) were studied using TGA TAQ500 with a heating

Table 2 Concentration and ratio of co-monomer, initiator used for WBMEs

Copolymer	Monomer composition in the feed		Mass of initiator (mol)	Total monomer (mol)
	Anililne hydrochloride (mass%)	Pyrrole (mass%)		
WBMEI	0	100	0.026	0.007
WBMEII	20	80	0.026	0.007
WBMEIII	40	60	0.026	0.007
WBMEIV	50	50	0.026	0.007
WBMEV	60	40	0.026	0.007
WBMEVI	80	20	0.026	0.007
WBMEVII	100	0	0.026	0.007

rate of $10\,°C \cdot min^{-1}$ under nitrogen. The morphology of copolymer microemulsion samples were studied with a Hitachi (S-3400N) scanning electron microscope (SEM). Microemulsions were spin coated at 2000 rpm over the stub, dried in vacuum, and viewed with a microscope after sputter-coating the samples with gold.

3 Results and Discussion

The TGA degradation curves obtained for SBME and WBME copolymers are presented in Figs. 1 and 2, respectively. The results indicate that SBMEVI and SBMEIV copolymers show a higher thermal stability than even the homopolymers prepared by the solvent-based microemulsion method. Comparisons of Figs. 1 and 2 indicate the influence of the method of preparation and solvent medium on the thermal stability of the copolymers. In WBME copolymers, polymers prepared with the co-monomer ratio containing 60 % aniline show a higher thermal stability than even the corresponding homopolymers (WBMEI and WBMEVII). In order to understand the influence of the preparation conditions on thermal stability, degradation temperatures for 5 %, 10 %, and 20 % thermal decompositions of the polymers are compared in Table 3. In general, the results show that WBMEs are always thermally less stable than the corresponding SBMEs. The thermal stability of SBME copolymers overlap with the trend followed by the degree of crystallinity [22,23] (Table 4) calculated from X-ray diffraction (XRD) data (Appendix) which influences the formation of ordered morphology.

Adding to the above, XRD data of WBMEs do not show characteristic peaks and therefore the degree of crystallinity could not be determined. It is interesting to note that the formation of ordered morphology has a strong influence on the thermal stability. Representative surface morphologies of the SBMEs and WBMEs are presented in Fig. 3 for comparison. SEM morphology of the solution containing an emulsifier and the oxidizing agent, spin-coated over the stub, is also used for comparison (See Appendix). It is interesting to note that SBMEVI (Fig. 3c), which shows a highly ordered nano-fiber morphology, shows the highest thermal stability at all temperatures. Even though SBMEIV shows a less index of crytallinity, high thermal stability is observed
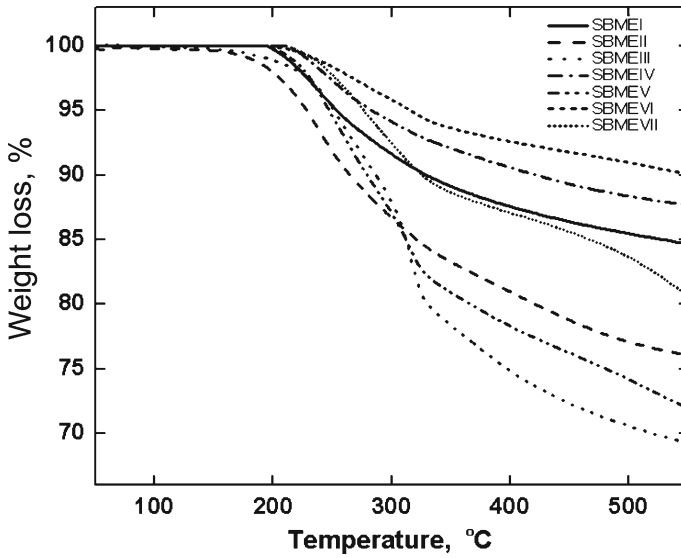
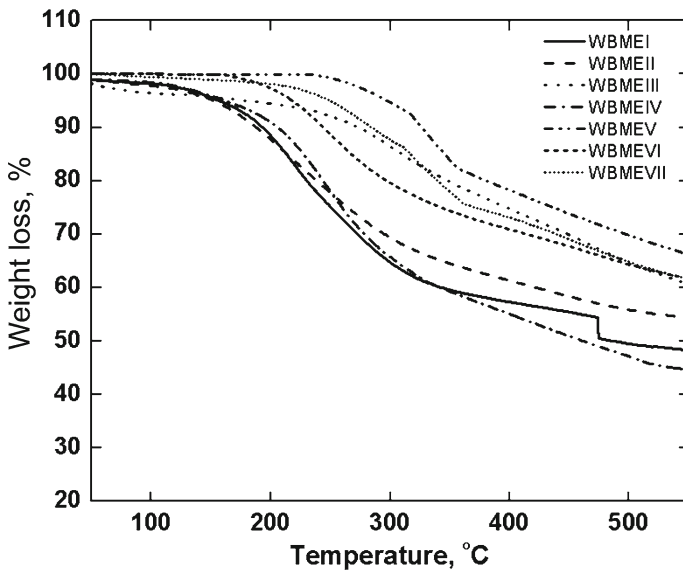**Fig. 1** TGA degradation curves obtained for SBME copolymers

Fig. 2 TGA degradation curves obtained for WBME copolymers

which can be attributed to the formation of a sheath-like multilayered structure. When the concentration of pyrrole is higher (SBMEI) (Fig. 3a), the resulting morphologies are granule-like with a regular spherical shape, without significant characteristic surface features. An increase in aniline in the feed ratio not only increases the granular size but also results in the formation of a random ordered sheath-like agglomerated

Table 3 Temperatures for different polymers at various percentages of degradation

Polymer	Temperature (°C) for degradation		
	5 %	10 %	20 %
SBMEI	253	326	605
SBMEII	228	265	421
SBMEIII	253	287	331
SBMEIV	281	422	550 (12.32 %)
SBMEV	246	280	367
SBMEVI	316	557	550 (9.94 %)
SBMEVII	277	327	560
WBMEI	158	194	231
WBMEII	153	188	239
WBMEIII	186	273	350
WBMEIV	161	207	245
WBMEV	298	326	382
WBMEVI	221	245	297
WBMEVII	253	285	337

For SBMEIV and SBMEVI, the stability is high, and at 550 °C, it does not reach 20 %

Table 4 Index of crystallinity calculated from XRD data

Copolymer	Index of crystallinity
SBMEI	0.482
SBMEII	0.283
SBMEIII	0.752
SBMEIV	0.517
SBMEV	0.847
SBMEVI	0.801
SBMEVII	0.639

structure as seen in the case of SBMEIV (Fig. 3b). Polyaniline prepared using the solvent-based microemulsion method shows less ordered and short micro-fibrils and shows a low index of crystallinity, which could be the reason for its low thermal stability compared to SBMEVI.

The morphology of the water-based emulsion shows a more ordered structure than its solvent-based counterpart which can be attributed to the ordered micelle formation of SDS in water. Unlike a solvent-based emulsion of pure PPy, the morphology formed by the water-based emulsion of PPy shows random nano-fibers with a three-dimensional network containing granules. The addition of aniline in the feed helps in the formation of hyper-branched cauliflower-like morphology, forming into coiled nano-fibers with granules of a smaller size (WBMEII) (Fig. 3e). The size of the

granule increases with an increase in the aniline concentration in the feed, which subsequently forms into three-dimensional networks with nano-fibers of increased length (WBMEV) (Fig. 3f). Because of the lengthy fibrous structures forming a network, the thermal stability of WBMEV may be higher. The low thermal stability of WBMEII can be attributed to the random arrangement. The featureless XRD data of WBMEs indicate that they are more amorphous and therefore when compared to SBMEs, WBMEs have poor thermal stability. Detailed studies on the morphology and XRD results are discussed in a previous publication [24].

The integral procedural decomposition temperature (IPDT) as proposed by Doyle provides a semi-quantitative means for comparison of relative thermal stabilities [25–27]. The integral procedural decomposition temperature is derived as a means of summing up the whole shape of the normalized data curve. IPDT accounts for the whole shape of the curve by measuring the area under the curve. The area under the curve divided by the total area is the total curve area, A^*, which is normalized with respect to both residual mass and temperature. A^* is converted to a temperature, T_{A^*} by

$$T_{A^*} = (T_{\text{end}} - T_{\text{ini}}) A^* + T_{\text{ini}} \tag{1}$$

T_{A^*} represents a characteristic end of the volatilization temperature rather than an IPDT having practical significance. The second curve area K^* is derived by drawing a rectangle relative to the x-axis up to T_{A^*}, and the y-axis mass fraction remaining at T_{A^*}. K^* is the ratio between the area under the curve (area under the curve up to T_{A^*}), to the total rectangular area up to T_{A^*}. The IPDT is determined by substituting K^* for A^* in Eq. 1. This index, the integral procedural decomposition temperature, is a reproducible datum having practical significance as an integrated half volatilization temperature. The calculated IPDT for different polymers is presented in Table 5. The SBME polymers (SBMEVII and SBMEVI) having a highly ordered nano-fiber structure show a higher IPDT and thermal stability. WBMES, WBMEV, and WBMEVII show a higher thermal stability, and the results overlap with other properties such as morphology, etc.

A knowledge of the kinetic parameters is one of the keys to determine the reaction mechanism of degradation. When changes in the mechanisms are observed, this can lead to unique thermal behavior and hence a better knowledge of the materials. The activation energy of different degradation stages for different copolymers is determined using the relation given by Doyle [28],

$$\ln(1 - C) = [-2.315(A/B)] + [0.4567(A/B)] [E_{\text{a}}/R(1/T)]. \tag{2}$$

where C is the amount of degraded polymer, E_{a} is the energy of activation, and A and B are constants. The activation energy of various degradation stages was calculated by plotting $\ln(1 - C)$ against $(1000/T)$. The representative relations obtained for SBMEI, VI, and VII are presented in Fig. 4. The tangent to the slope of the $\ln(1 - C)$ versus $1/T$ plot over various intervals of the data was used to interpret the complicated decomposition of the polymers, and these tangents were used to calculate the effective activation energies for these temperature regimes [29]. The energies of activation
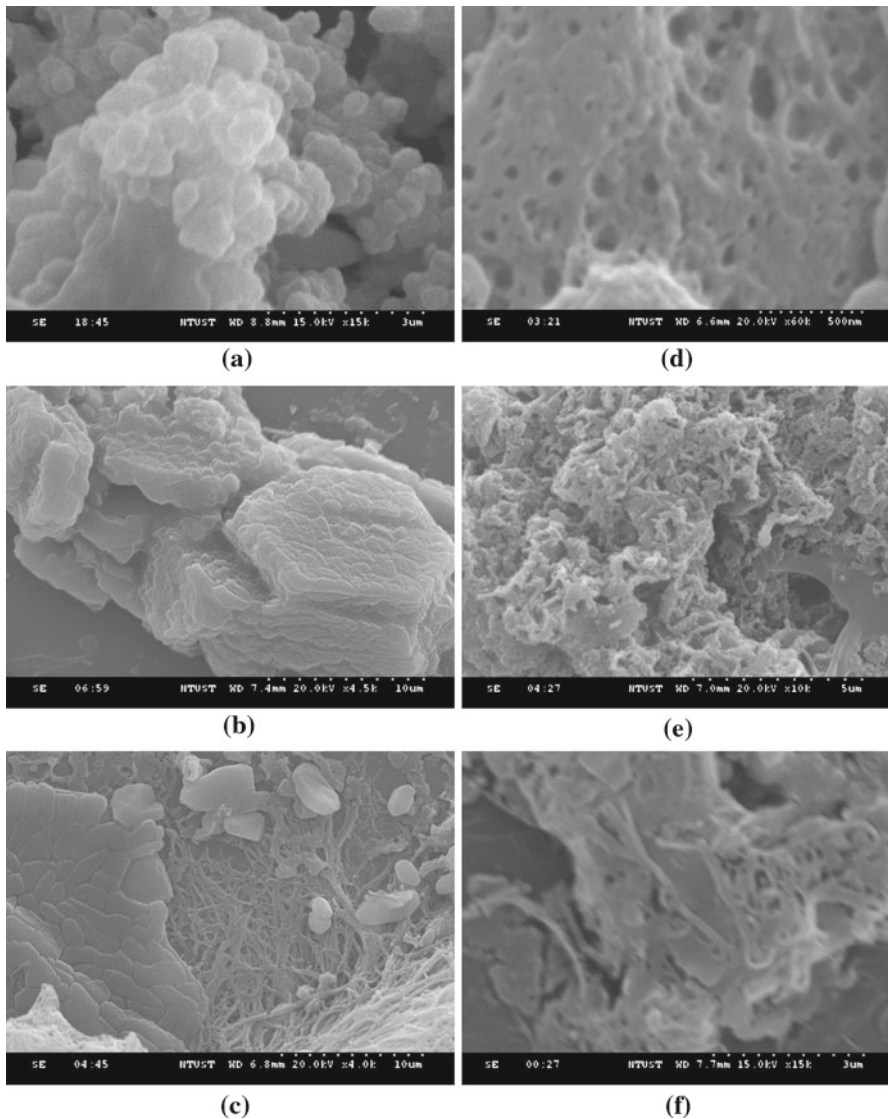
Fig. 3 SEM Morphology of different copolymers: (**a**) SBMEI, (**b**) SBMEIV, (**c**) SBMEVI, (**d**) SBMEVII, (**e**) WBMEII, and (**f**) WBMEV

obtained for different copolymers for various stages of degradation are presented in Table 6.

In general, SBME copolymers degrade by a three-stage process, while WBME copolymers degrade in four stages. Of all the copolymers, SBMEIV, which shows a higher thermal stability, degrades by a single-stage process and the degradation starts only at 210 °C. It is interesting to note that many of the SBME copolymers show high thermal stability around 200 °C (Table 5), whereas WBMEs degrade even at lower

Table 5 IPDT values obtained for different polymers

Polymer	IPDT (K)
SBMEI	547
SBMEII	524
SBMEIII	530
SBMEIV	533
SBMEV	518
SBMEVI	552
SBMEVII	577
WBMEI	475
WBMEII	453
WBMEIII	545
WBMEIV	491
WBMEV	591
WBMEVI	461
WBMEVII	546
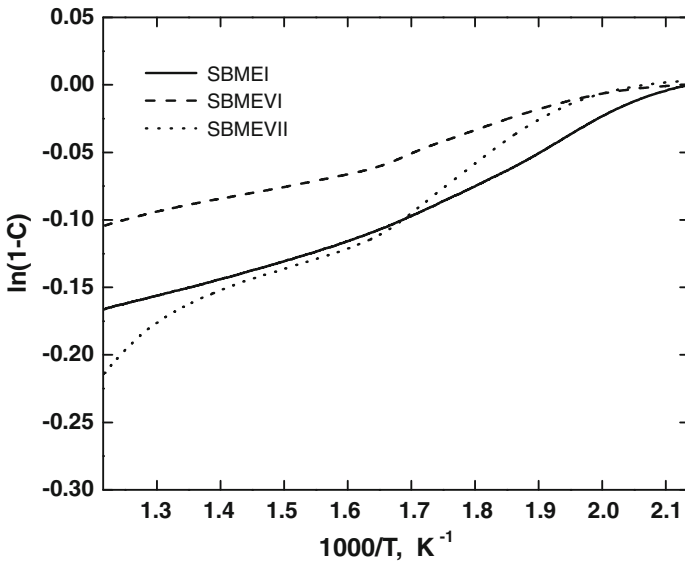
Fig. 4 $\ln(1 - C)$ against $1000/T$ for SBMEI, SBMEVI, and SBMEVII

temperatures except for WBMEV and WBMEVII which are stable up to 228 °C and 153 °C, respectively. In WBME copolymers, the addition and increase in aniline in the copolymer relative to pyrrole result in a decrease of the stability (decrease of E_a for the first two stages of degradation) for up to 50 % of aniline in the co-monomer ratio. It is also interesting to note that the addition of pyrrole to polyaniline (WBMEVII) increases the stability at the first two stages of degradation with an increase in

Table 6 Energy of activation calculated obtained from TGA curves for different copolymers

Polymer	Temp. range (K)	E_a (kJ · mol^{-1} · K^{-1})	Polymer	Temp. range (K)	E_a (kJ · mol^{-1} · K^{-1})
SBMEI	468–638	19.934	WBMEI	323–384	13.098
	638–823	16.635		384–462	15.823
				462–575	19.255
				575–769	15.329
				769–823	16.606
SBMEII	323–464	13.630	WBMEII	323–444	12.943
	464–764	19.168		444–607	18.075
	764–823	14.647		607–823	16.472
SBMEIII	323–489	14.756	WBMEIII	323–472	11.101
	489–598	20.309		472–545	17.117
	598–823	17.167		545–823	21.926
SBMEIV	483–823	19.699	WBMEIV	323–395	12.010
				395–451	15.714
				451–603	18.979
				603–791	18.259
				791–823	14.220
SBMEV	466–598	20.574	WBMEV	501–630	23.471
	598–823	18.272		630–823	22.391
SBMEVI	470–604	20.696	WBMEVI	323–459	16.907
	604–823	18.644		459–487	18.900
				487–619	19.917
				619–823	19.189
SBMEVII	483–605	21.148	WBMEVII	426–508	14.580
	605–767	18.280		508–585	20.792
	767–823	25.505		585–635	22.625
				635–823	20.951

the activation energy. WBMEV which has 60 % of aniline in the feed ratio shows a higher thermal stability than even the WBME homopolymers. In SBME copolymers, the addition of aniline to pyrrole increases the temperature of the first stage of degradation. Overall, the values of the activation energy of the first stage of degradation in SBMEs follow the trend of the index of crystallinity relation and the highest stability in the first stage of degradation is observed for SBMEIV. An SBMEVI copolymer, which has a highly ordered morphology and crystallinity, shows higher activation energy at all stages of degradation.

It has been shown that in polyanilines [30–32], which degrade by the three-stage process, the first stage of degradation can be due to the loss of moisture, free HCl, and unreacted monomer while the second stage may be attributed to loss of dopants from deeper sites in the material. Polyaniline backbone degradation occurs at the third stage. Copolymers prepared using a water-based microemulsion will have more residual and bound water, suggesting a higher proportion of low molar mass fractions. Therefore, during the first and second stages of degradation, the mass loss is high compared to SBMEs. Copolymers containing comparatively equal amounts (WBMEs) of co-monomers in the feed show a higher thermal stability. It is interesting to note that even though the temperature range of the first degradation in SBMES is higher when compared to WBMEs, copolymers with a comparable ratio of pyrrole and aniline prepared from water-based microemulsions show a higher thermal stability signifying very low degradation up to 200 °C.

It has been shown [33] that in polypyrrole prepared with $FeCl_3$, a greater number of PPy chains will be formed and consequently, the inter-chain interaction probability will be enhanced. This may materialize through possible H-bonding between the N heteroatoms of a PPy chain and the pyrrolic H atoms of another such chain. This situation will imply higher matrix stability as revealed by the thermal stability trend. Excess $FeCl_3$ may act as a dopant, leading to charge–transfer interactions with the N heteroatoms in the PPy chain. This would tend to reduce the extent of interchain H-bonding ultimately showing less thermal stability. This has been clearly reflected in the case of copolymers of WBMEs in the earlier stages of degradation.

4 Conclusions

Copolymers of pyrrole and aniline were prepared using water- and solvent-based microemulsion methods. The co-monomer ratio of the binary mixture of the monomers was changed, and the effect of the above on thermal degradation was studied in detail. The overall results obtained from the above studies show that the monomer composition and the polymerization environment affects the morphology and the order of crystallinity. This in turn affects the thermal degradation, the energy of activation, and the stages of degradation apart from the enthalpy of transition and transition temperatures.
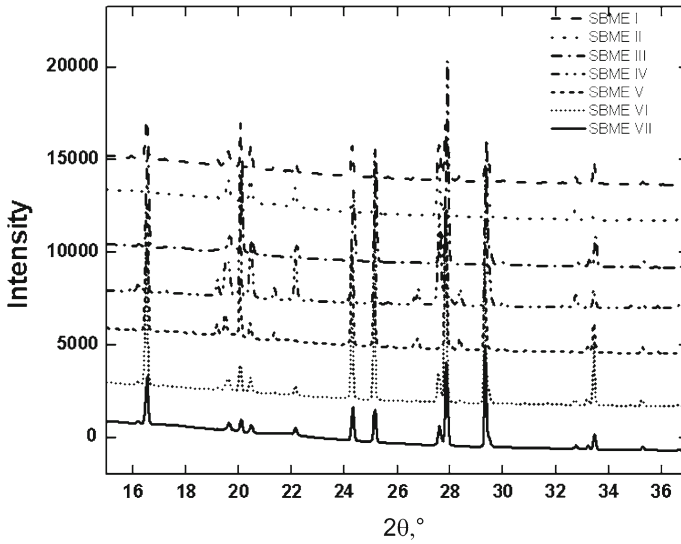
Appendix

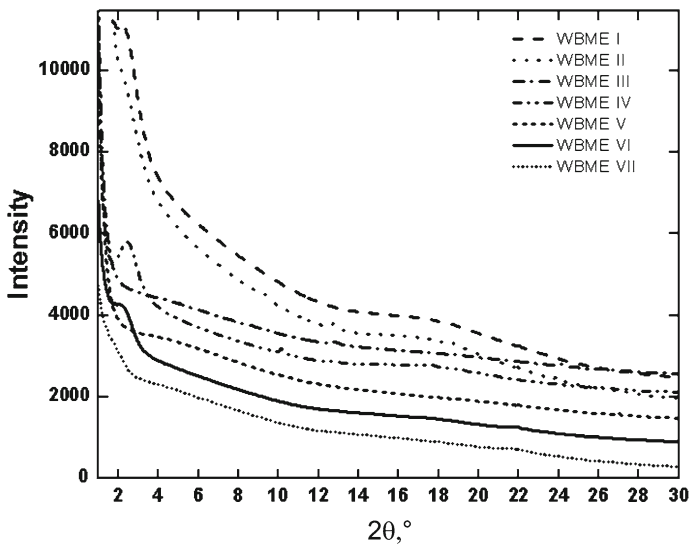**Fig. A1** XRD patterns of different SBME copolymers
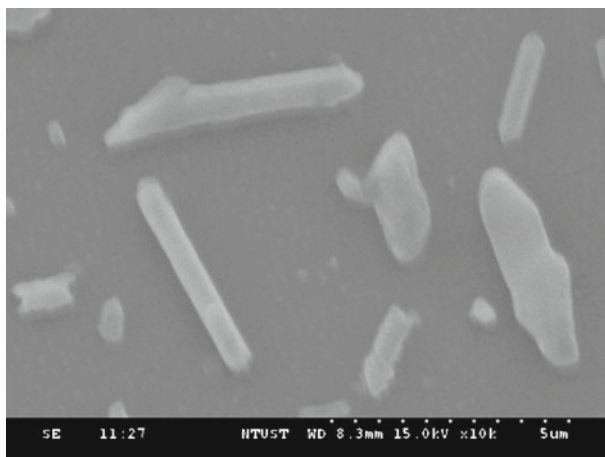

Fig. A2 XRD patterns of WBME copolymers

Fig. A3 SEM morphology of control experiments containing solvents with initiator/emulsifier (without monomer/polymer)

References

1. S. Xing, C. Zhao, T. Zhou, S. Jing, Z. Wang, J. Appl. Polym. Sci. **104**, 3523 (2007)
2. H. Bai, O. Chen, C. La, C. Shi, Polymer **48**, 4015 (2007)
3. C.H. Cho, H.J. Choi, J.W. Kim, M.S. Jhon, J. Mater. Sci. **39**, 1883 (2004)
4. G. Cakmak, G. Kucukyavaz, Z. Kuchkyavuz, Synth. Met. **151**, 10 (2005)
5. M. Karakisla, L. Aksu, M. Sacak, Polym. Int. **51**, 1371 (2002)
6. C. He, C. Yang, Y. Li, Synth. Met. **139**, 539 (2003)
7. F. Yan, C. Zheng, X. Zhai, D. Zhao, J. Appl. Polym. Sci. **67**, 747 (1998)
8. S.E. Webber, J. Phys. Chem. B **102**, 2618 (1998)
9. J. Stejskal, M. Omastova'b, S. Fedorovac, J. Prokesd, M. Trchovaa, Polymer **44**, 1353 (2003)
10. S. Palaniappan, Polym. Adv. Technol. **13**, 54 (2002)
11. P.S. Rao, S. Subrahmanya, D.N. Sathyanarayana, Synth. Met. **128**, 311 (2002)
12. P.S. Rao, D.N. Sathyanarayana, S. Palaniappan, Macromolecules **35**, 4988 (2002)
13. S. Palaniappan, S. Lakshmi Devi, Polym. Degrad. Stabil. **91**, 2415 (2006)
14. P.C. Rodrigues, G.P. De Souza, J.D. Da Motta Neto, L. Akcelrued, Polymer **43**, 5493 (2002)
15. G. Inzelt, J. Electroanal. Chem. **279**, 169 (1990)
16. M.K. Traore, W.T.K. Stevenson, B.J. McCormick, R.C. Dorey, W. Shao, D. Meyers, Synth. Met. **40**, 137 (1991)
17. S. Palaniappan, B.H. Narayana, Thermochim. Acta **237**, 91 (1994)
18. P.S. Abthagir, R. Saraswathi, Mater. Chem. Phy. **92**, 21 (2005)
19. V.T. Truong, J.G. Ternan, Polymer **36**, 905 (1995)
20. T.C. Wen, S.L. Hung, M. Digar, Synth. Met. **118**, 11 (2001)
21. D. Mecerreyes, R. Stevens, C. Nguyen, J.A. Pomposo, M. Bengoetxea, H. Grande, Synth. Met. **126**, 173 (2002)
22. B.R. Manjunath, A. Venkataraman, T.J. Stephen, J. Appl. Polym. Sci. **17**, 1091 (1973)
23. S. Saravanan, C.J. Mathai, N.R. Anantharaman, S. Venkatachalam, P.V. Prabhakaran, J. Phys. Chem. Solids **67**, 1496 (2006)
24. A. Prasannan, N. Somanathan, P.D. Hong, W.T. Chuang, Mater. Chem. Phy. **116**, 406 (2009)
25. C.D. Doyle, Anal. Chem. **33**, 77 (1961)
26. G. Sumana, D.C. Gupta, J. Polym. Mater. **21**, 259 (2004)
27. S. Radhakrishnan, N. Somanathan, T. Narashimhaswamy, M. Thelakkat, H.W. Schmidt, J. Therm. Anal. Calorim. **85**, 433 (2006)
28. C.D. Doyle, J. Appl. Polym. Sci. **5**, 285 (1961)

29. S. Radhakrishnan, N. Somanathan, M. Thelakkat, Int. J. Thermophys. **30**, 1074 (2009)
30. F. Yan, G. Xue, J. Mater. Chem. **9**, 3035 (1999)
31. R. Ansari, M.B. Keivani, E-J. Chem. **3**, 202 (2006)
32. N. Chandrakanthil, M.A. Careem, Polym. Bull. **44**, 101 (2000)
33. M. Biswas, A. Roy, J. Appl. Polym. Sci. **51**, 15785 (1994)